ELSEVIER

Catalysis Today 78 (2003) 499–505

CATALYSIS TODAY

www.elsevier.com/locate/cattod

Hydrotreating properties of mixed $Nb_xMo_{1-x}S_2$ alumina supported catalysts

V. Gaborit [a], N. Allali [a], M. Danot [a], C. Geantet [b,*], M. Cattenot [b], M. Breysse [c], F. Diehl [d]

[a] *Laboratoire de Chimie des Solides, IMN, UMR 6502, CNRS-Université de Nantes, 2 rue de la Houssinière, BP 32229, 44322 Nantes Cedex 3, France*

[b] *Institut de Recherches sur la Catalyse, CNRS, 2 Avenue Albert-Einstein, 69626 Villeurbanne Cedex, France*

[c] *Laboratoire de Réactivité de Surface, Univ. P&M Curie (Paris VI, tour 54-2ème étage), 4 Place Jussieu, 75252 Paris Cédex 05, France*

[d] *Institut Français du Pétrole, Division Cinétique et Catalyse, 1 et 4 Avenue de Bois Préau, 92852 Rueil-Malmaison, France*

Abstract

Niobium-molybdenum disulfide solid solution ($Nb_xMo_{1-x}S_2$) has been prepared in a dispersed state on gamma alumina. The existence of this solid solution supported on alumina carrier has been proven with the help of EXAFS technique. The catalytic properties of these materials have been studied in hydrogenation and hydrodesulfurization reactions. Interestingly, as already observed for niobium sulfide, the activity of the $Nb_xMo_{1-x}S_2$ solid solution (HDS of DBT, $P_{tot} = 33$ bar) is not decreased in the presence of H_2S up to $p(H_2S) = 200$ Torr, at least up to $x = 0.4$.

Keywords: Alumina-supported catalysis; Hydrotreating catalysts; EXAFS technique

1. Introduction

Present and future regulations [1] concerning the emission of SO_x and NO_x gas are animating the research in both fields of formulation of hydrotreating catalysts and design of new processes. In fact, conventional alumina-supported CoMo, NiMo and NiW sulfide hydrotreating catalysts are not sufficiently effective for an exhaustive heteroatom removal. New active systems are now required and the interest for the hydrotreating properties of noble metals, carbides or nitrides, or new sulfide phases has considerably grown during the last years [2].

Systematic studies performed on unsupported catalysts revealed that sulfides other than the conventional CoMoS, NiMoS, and NiWS, such as noble metal sulfides (RuS_2, Rh_2S_3) or niobium sulfides ($Nb_{(1-x)}S$, NbS_2, NbS_3) are potentially good candidates for new formulations of hydrotreating catalysts. Moreover, niobium and tantalum sulfides present unique acidic properties and therefore enhance the formation of cracking and isomerisation products [3,4].

Supported niobium sulfides were found to be more active than molybdenum disulfide supported catalysts with an equivalent active phase loading, despite their poorer dispersion. Small amounts of Nb added to a commercial NiMo catalysts provided a slight enhancement of catalytic activity and an improvement in the acidic properties [5]. As for Mo-based catalysts,

* Corresponding author. Tel.: +33-472-44-5336; fax: +33-472-44-5399.
E-mail address: geantet@catalyse.univ-lyon1.fr (C. Geantet).

0920-5861/02/$ – see front matter
PII: S0920-5861(02)00336-X

we can expect that addition of a dopant to niobium sulfides could induce a synergetic effect or/and an improvement of the active phase dispersion. However, attempts to dope carbon-supported niobium sulfides with Ni did not allow significant synergetic effect to be observed [6]. Consequently, the present research was orientated in a different way and aimed to prepare a well-defined mixed Nb-containing disulfide in a well-dispersed state. In addition to dispersion effects, introduction of another cation in the niobium sublattice of NbS_2 could be expected to induce a modification of the electronic properties of the solid (M–S bond strength) and subsequent effects on the sulfidation and activity. Similar approach was successful in the case of the RuS_2 pyrite structure: $Ni_xRu_{1-x}S_2$ solid solution particles could be dispersed on the surface of alumina and an enhancement of the hydrogenation properties of the catalysts was observed as compared to the catalytic actitivities of the individual sulfides [7]. Due to the well-known catalytic properties of molybdenum, we thought it could be interesting to involve this cation, along with niobium, in mixed disulfide supported catalysts. The Nb–Mo system could be expected to allow formation of a $Nb_xMo_{1-x}S_2$ solid solution since, in their simple disulfides MoS_2 and NbS_2, molybdenum and niobium both sit in trigonal prismatic sulfur environment. Besides, comparison of the cell parameters of the 2H varieties ($a MoS_2 = 3.161$ Å and $a NbS_2 = 3.32$ Å; $c MoS_2 = 12,298$ Å and $c NbS_2 = 11.94$ Å) shows that the geometrical characteristics of the $[MS_2]$ layers do not differ a lot, which is another favorable feature for the obtention of the alumina-supported $Nb_xMo_{1-x}S_2$ solid solution to be possible.

2. Experimental

2.1. Catalyst preparation

A series of mixed Nb–Mo catalysts ($Nb_{1-x}Mo_x$, $0 < x < 1$) were prepared by impregnation of γ-alumina with successively ammonium heptamolybdate and niobium oxalate solutions. Total cation loading was kept constant (Mo + Nb = 10% with respect to the support mass). Chemical analysis confirmed the deposition of the expected amount of metals. The sample was then allowed to dry at room temperature. Higher drying temperatures (e.g. 373 K) cannot be used because, after such a treatment, niobium cannot be correctly sulfurized at moderate temperature. Sulfurization was performed at 673 K for 4 h at high pressure under batch conditions using CS_2 as the sulfurizing agent [8]. A commercial NiMo catalyst was used as a reference catalyst (2 wt.% of Ni and 9 wt.% of Mo).

2.2. Reaction test

The catalysts were tested by means of two reactions: hydrodesulfurization of dibenzothiophene (HDS of DBT) and hydrogenation of tetralin. Experiments were carried out in vapour phase in microreactors running in dynamic mode. The operating conditions, depending on the nature of the reacting molecule, are listed in Table 1. For the study of the influence of H_2S on the activity in HDS of DBT, $p(H_2S)$ was varied from 0 to 27 kPa.

According to the model of the integral reactor, the rate constant k of a reaction can be expressed as follows:

$$k = \frac{F_0}{mC_0}\ln(1-x) \quad (\mathrm{l/s\,g^{-1}})$$

where x is the conversion, m the mass of catalyst (g), F_0 the molar flow of reactant (mol/s), and C_0 the concentration of reactant (mol/l).

When the conversion is less than 15%, the above formula can be simplified, giving the reaction rate:

$$r = \frac{F_0}{m}x \quad (\mathrm{mol/s\,g^{-1}})$$

The activities were measured when the steady state of the catalyst was reached, i.e. after 15 h on-stream. Activity measurement accuracy is within 10%.

Table 1
Operating conditions of the catalytic tests

Reaction	Temperature (K)	Total pressure (Pa)	Reactant partial pressure (Pa)
HDS of DBT	523	30×10^5 [a]	577
Hydrogenation of tetralin	623	43×10^5 [a]	8886

[a] H_2S was added to the H_2 flow: from 0 to 0.8 vol.% in the DBT HDS experiments, and 2 vol.% in the tetralin hydrogenation ones.

2.3. X-ray absorption

EXAFS spectra were recorded at LURE on the EXAFS 1 and 2 spectrometers, using a Si(3 1 1) channel cut monochromator. During the experiments, the storage ring (DCI) used 1.85 GeV positrons with an average intensity of 250 mA. Samples were prepared under inert atmosphere by sandwiching the powders between two X-ray transparent adhesive tapes (Kapton). Data were recorded in transmission mode and measurements performed at the Mo K-edge from 19 850 to 20 800 eV and at the Nb K-edge from 18 850 to 19 800 eV. Data processing was performed with the package developed by Michalowicz [9]. Amplitude and phase of backscattering as well as mean-free-path were taken from FEFF codes [10].

2.4. Electron microscopy

Catalyst grains were dispersed in pure ethanol, the suspension stirred in an ultrasonic bath and one drop deposited on a carbon coated copper grid. These grains were examined in a JEOL 2010 device equipped with a Link-Isis EDX detector. For statistical study of the dispersion, length and stacking were determined for more than 600 sulfide particles for each sample [11]. Various probe sizes ($2.5 < \phi < 10$ nm) were used for EDX analyses.

3. Results and discussion

3.1. Structural characterization

Due to the sulfide crystallite size X-ray diffraction could not provide any valuable structural information and it is the EXAFS technique which allowed the alumina-supported sulfide nanoparticles to be identified as a $Nb_xMo_{1-x}S_2$ solid solution rather than two-phase ($MoS_2 + NbS_2$) systems. It has first to be noticed that, due to the presence of the van der Waals gap, EXAFS is only sensitive to the intra-layer neighboring of the absorbing atom [12]. Figs. 1 and 2 show the radial distribution functions obtained at the Nb and Mo K-edges, respectively. Structural data obtained from the fitting of the imaginary part of the Fourier transforms are given in Tables 2 and 3 for the Nb and Mo K-edges, respectively. The first peak cor-

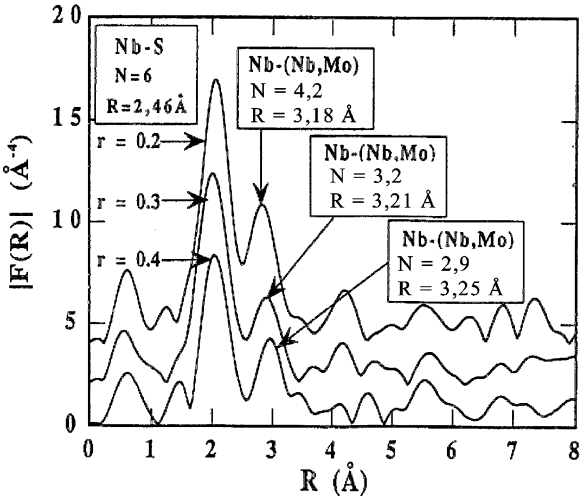

Fig. 1. Radial distribution function at the Nb K-edge for various $Nb_xMo_{1-x}S_2/Al_2O_3$ samples.

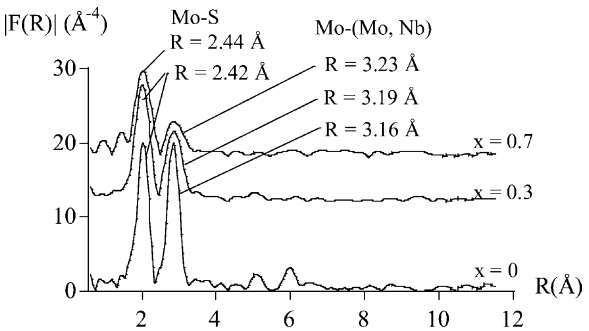

Fig. 2. Radial distribution function at the Mo K-edge for various $Nb_xMo_{1-x}S_2/Al_2O_3$ samples.

Table 2
Nb K-edge EXAFS analysis: structural parameters of $Nb_xMo_{1-x}S_2/Al_2O_3$ samples with various compositions

$Nb_xMo_{1-x}S_2$	$x = 0.2$	$x = 0.3$	$x = 0.4$
N_1	6.0	4.5	4.0
R_1 (Å)	2.45	2.45	2.48
σ_1 (Å)	5×10^{-2}	5×10^{-2}	6×10^{-2}
ΔE_1 (eV)	1	2	4
N_2	4.2	3.2	2.9
R_2 (Å)	3.18	3.21	3.25
σ_2 (Å)	7×10^{-2}	7×10^{-2}	6×10^{-2}
ΔE_2 (eV)	−10	−5	−8

Table 3
Mo K-edge EXAFS analysis: structural parameters of $Nb_xMo_{1-x}S_2/Al_2O_3$ with various compositions

$Nb_xMo_{1-x}S_2$	$x = 0.0$	$x = 0.3$	$x = 0.7$
N_1	6.0	5.1	3.9
R_1 (Å)	2.42	2.42	2.44
σ_1 (Å)	4×10^{-2}	5×10^{-2}	5×10^{-2}
ΔE_1 (eV)	6	3	4
N_2	6.0	2.5	2.0
R_2 (Å)	3.16	3.19	3.23
σ_2 (Å)	3×10^{-2}	4×10^{-2}	6×10^{-2}
ΔE_2 (eV)	1	0	−3

responds to the six sulfur nearest neighbors expected for a lamellar disulfide such as MoS_2 or NbS_2, even if the refined neighbor numbers can be reduced by disorder, this effect being found to increase with the niobium amount. The second peak reflects the in-plane cationic neighborhood of the absorbing element. In a two-phase system ($MoS_2 + NbS_2$), niobium would have only niobium neighbors and molybdenum only molybdenum ones. In a $Nb_xMo_{1-x}S_2$ solid solution, both niobium and molybdenum absorbers would have niobium and molybdenum neighbors. Unfortunately, due to their relative positions in the periodic table, niobium and molybdenum have very similar backscattering amplitudes and phase shifts, and EXAFS cannot thus allow these two backscatterers to be distinguished. However, fortunately, the M–M distances in MoS_2 and NbS_2 are sufficiently different (Mo–Mo = 3.16 Å in MoS_2 and Nb–Nb = 3.32 Å in NbS_2) for the intercationic distances in the mixed systems to be informative. Effectively, it can be seen (Tables 2 and 3) that the distance between the absorbing atom (Mo or Nb) and its cationic neighbors increases with the niobium amount. It means that both Mo and Nb are present in the in-plane cationic environment of the probe cation and that, as it could be expected, the niobium contribution increases with x, since d(Nb–Nb) > d(Mo–Mo). In other words, every [MS_2] layer contains both Nb and Mo cations and can thus be formulated as [$Nb_xMo_{1-x}S_2$]. Kadijk [13] previously prepared highly crystalline unsupported $Nb_xMo_{1-x}S_2$ solid solution and evidenced an evolution of the cell parameters with x. Fig. 3 allows to compare the distances we refined to the value reported by Kadijk for the a crystallographic parameter (which corresponds

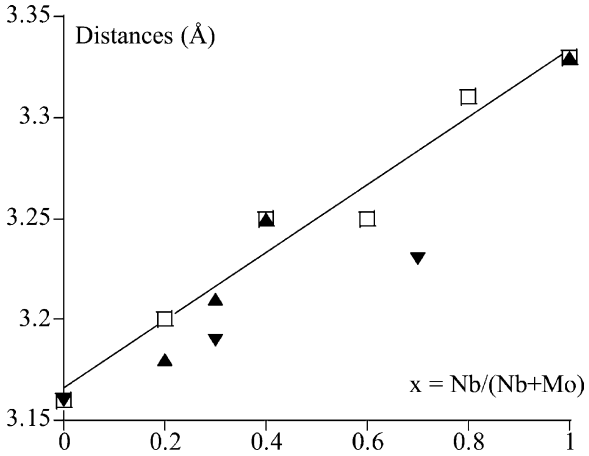

Fig. 3. Comparison of our EXAFS refined Mo–(Nb,Mo) (▼) and Nb–(Nb,Mo) (▲) distances to the a parameter (□) obtained from XRD for highly crystalline unsupported $Nb_xMo_{1-x}S_2$ [13] (the linear fitting of these a values is approximate since the structure shifts from 2H to 3R around $x = 0.5$).

to the cation–cation distance) of his solid solution. The same trend is observed corresponding roughly to a Vegard's law. All these facts show that we obtained an alumina-supported $Nb_xMo_{1-x}S_2$ intra-layer solid solution.

3.2. Dispersion

A TEM picture of the sample with $x = 0.4$ is shown in Fig. 4. The characteristic lamellar structure of MS_2 layered sulfides is observed. Average length and stacking are smaller ($l_{av} = 6.1$ and $n_{av} = 4.3$) as compared to NbS_2/Al_2O_3 samples for which particles with l up to 80 nm and n up to 20 could be observed. EDX analysis evidences that the Nb and Mo elements are homogeneously distributed whatever the probe size used.

3.3. Catalytic properties

The catalytic properties of the series of catalysts were evaluated at first in tetralin hydrogenation. Fig. 5 shows that the activity increases almost linearly with the Nb content. No synergetic effect then occurs but for the $x = 0.4$ sample the catalytic activity is slightly better than expected on the basis of a linear evolution from MoS_2 and NbS_2, which can be related to better dispersion of the nanoparticles. According to

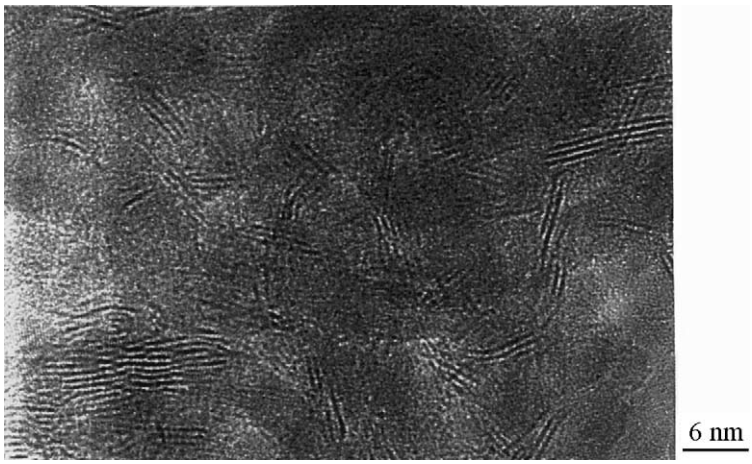

Fig. 4. TEM image of a $Nb_xMo_{1-x}S_2/Al_2O_3$ sample ($x = 0.4$).

the reaction scheme for the transformation of tetralin, acidic sites might be involved in the formation of methyl indan and decalin isomers [14,15]. Selectivity for formation of these products can thus be used to estimate the acidic strength of a catalyst. In our case, we observed an increase of these acidic properties, the NbS_2 ($x = 1$) being seven times more acidic than MoS_2 ($x = 0$) and intermediate acidities for the mixed catalysts. Therefore, a tailoring of the acidic properties is offered by the use of such mixed system. Fig. 6 shows the influence of the H_2S pressure on the conversion of dibenzothiophene for a NiMo industrial catalyst and two alumina-supported

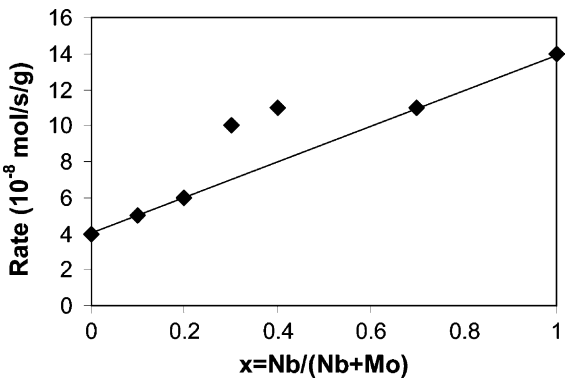

Fig. 5. Activity of a series of alumina-supported $Nb_xMo_{1-x}S_2$ catalysts in tetralin conversion at 623 K.

niobium-containing catalysts: NbS_2 and $Nb_xMo_{1-x}S_2$ ($x = 0.4$). As already observed for unsupported catalysts [3,4], Nb sulfide-based catalysts are insensitive to H_2S pressure, whereas conventional catalysts are strongly inhibited by small H_2S amounts, their activity remaining then stable if the H_2S pressure is increased. The $Nb_xMo_{1-x}S_2$ mixed sample presents the same behavior as the Nb catalysts and, if at low H_2S pressure it is less active than a conventional NiMo catalyst, it becomes more active at higher H_2S pressure. According to kinetic studies, the behavior observed for conventional sulfide catalysts (two domains: inhibition and then stabilization) either for hydrogenation or HDS is attributed to two different rate determining steps [16,17]. When the catalytic activity does not depend on the H_2S partial pressure, it is assumed that the rate determining step corresponds to the attack of the reactant by a base (S^{2-} species for instance). In the case of Nb-based sulfide catalysts, this mechanism is apparently the only one to be involved which evidences the specificity of the catalytic sites present in these systems. Theoretical calculations evidences that NbS_2 belongs to the high bond strength side of the well known volcano curve which correlates bond strength with catalytic activity [18]; sensitivity of MoS_2 or Co doped MoS_2 surfaces to H_2/H_2S pressure were also computed [19,20]. Such a theoretical approach will be helpful for the understanding of NbS_2 and mixted $Nb_{1-x}Mo_x$ system.

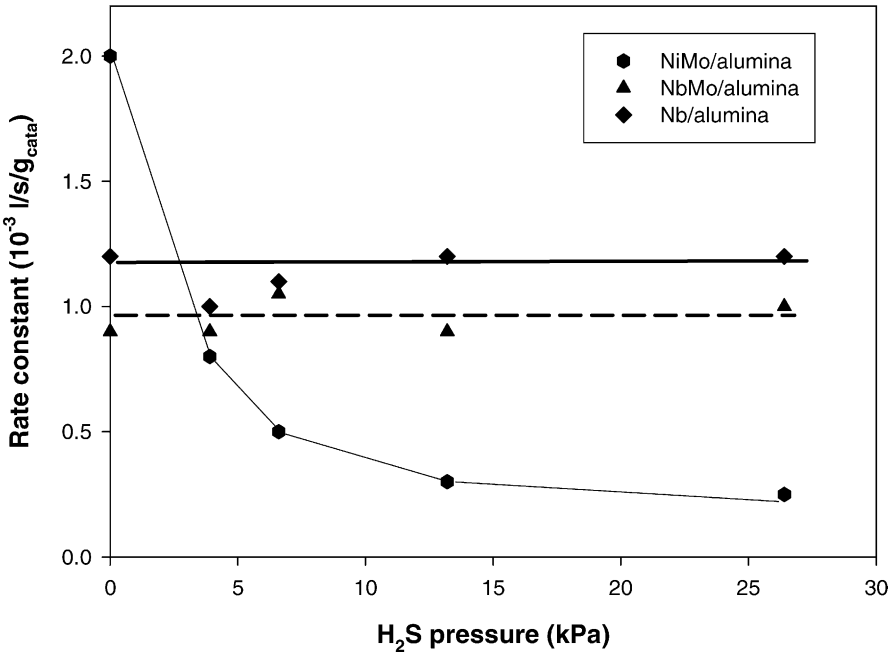

Fig. 6. Effect of the H_2S partial pressure on the activity of a commercial NiMo catalyst, NbS_2/Al_2O_3, and $Nb_xMo_{1-x}S_2/Al_2O_3$ ($x = 0.4$) in HDS of DBT.

4. Conclusion

The existence of the solid solution $Mo_xNb_{1-x}S_2$ in nanoparticles was for the first time evidenced by EXAFS. As compared to NbS_2, the solid solution provides a better dispersion of the particles but does not show any synergetic effect. As the consequence $Mo_xNb_{1-x}S_2$ with $x = 0.4$ was considered as the best catalyst for the series studied. As compared to conventional NiMo catalysts, supported $Mo_xNb_{1-x}S_2$ ($x = 0.4$), like NbS_2, are insensitive to H_2S partial pressure suggesting good capabilities for the conversion of high sulfur loaded gas oils.

Acknowledgements

This work was carried out in the framework of the contract “Hydrodésulfuration des Gazoles”. It received support from Elf-Antar, IFP, Procatalyse, Total, Ecotech-CNRS.

References

[1] Off. J. Eur. Commun. L350 (1998) 58.
[2] B.S. Clausen, H. Topsoe, F.E. Massoth, in: J.R. Anderson, M. Boudart (Eds.), Catalysis Science and Technology, vol. 11, Springer, Berlin, 1996.
[3] M. Lacroix, N. Boutarfa, C. Guillard, M. Vrinat, M. Breysse, J. Catal. 120 (1989) 473.
[4] M. Vrinat, C. Guillard, M. Lacroix, M. Breysse, M. Kurdi, M. Danot, Bull. Soc. Chim. Belg. 96 (1987) 1017.
[5] C. Geantet, V. Gaborit, N. Allali, M. Cattenot, M. Breysse, M. Vrinat, M. Danot, Catal. Today 57 (2000) 267–273.
[6] V. Gaborit, Ph.D. Université de Nantes, 1998.
[7] J.A. De Los Reyes, M. Vrinat, C. Geantet, M. Breysse, J. Grimblot, J. Catal. 142 (1993) 455.
[8] N. Allali, A.M. Marie, M. Danot, C. Geantet, M. Breysse, J. Catal. 156 (1995) 279.
[9] A. Michalowicz, in: J. Goulon, C. Goulon-Ginet, N.B. Brookes (Eds.), Proceedings of the Ninth International Conference on X-ray Absorption Fine Structure, vol. I, Ed. de Physique, 1997, pp. C2–235.
[10] J. Rehr, J. Mustre de Leon, S.I. Zabinsky, R.C. Albers, J. Am. Chem. Soc. 113 (1991) 5135.
[11] B. Imelik, J.C. Vedrine (Eds.), Catalyst Characterization: Physical Techniques for Solid Materials, Plenum Press, New York, 1994, p. 509.

[12] C. Calais, N. Matsubayashi, C. Geantet, Y. Yoshimura, H. Shimada, A. Nishijima, M. Lacroix, M. Breysse, J. Catal. 174 (1998) 130.
[13] F. Kadijk, Ph.D. University of Groningen, 1969.
[14] M. Mahouer, J.L. Lamberton, G. Perot, Catal. Today 29 (1996) 241.
[15] V. Gaborit, N. Allali, C. Geantet, M. Breysse, M. Vrinat, M. Danot, Catal. Today 57 (2000) 267.
[16] S. Kasztelan, D. Guillaume, Ind. Eng. Chem. Res. 2 (33) (1994) 203.
[17] E. Olguin Orozco, M. Vrinat, Appl. Catal. A 170 (1998) 195.
[18] H. Toulhoat, P. Raybaud, S. Kasztelan, G. Kresse, J. Hafner, Catal. Today 50 (1999) 629.
[19] P. Raybaud, J. Hafner, G. Kresse, S. Kasztelan, H. Toulhoat, J. Catal. 189 (2000) 129.
[20] P. Raybaud, J. Hafner, G. Kresse, S. Kasztelan, H. Toulhoat, J. Catal. 190 (2000) 128.